Journal of Astronomical Telescopes, Instruments, and Systems

AstronomicalTelescopes.SPIEDigitalLibrary.org

Noncontact temperature estimation method on the actively cooled primary mirror surface of large ground-based solar telescope

Yangyi Liu
Naiting Gu
Changhui Rao

SPIE.

Yangyi Liu, Naiting Gu, Changhui Rao, "Noncontact temperature estimation method on the actively cooled primary mirror surface of large ground-based solar telescope," *J. Astron. Telesc. Instrum. Syst.* **3**(4), 046001 (2017), doi: 10.1117/1.JATIS.3.4.046001.

Noncontact temperature estimation method on the actively cooled primary mirror surface of large ground-based solar telescope

Yangyi Liu,[a,b] Naiting Gu,[a,b] and Changhui Rao[a,b,*]
[a]Chinese Academy of Sciences, Key Laboratory on Adaptive Optics, Chengdu, China
[b]Chinese Academy of Sciences, Key Laboratory on Adaptive Optics, Institute of Optics and Electronics, Chengdu, China

Abstract. To control the mirror seeing effect and the thermal deformation, the actively cooled primary mirror is utilized in a large ground-based solar telescope. Due to direct solar illumination and high reflectivity of the mirror surface coating, the traditional contact or noncontact temperature measuring methods of the mirror surface are not available. A noncontact temperature estimation method based on the analytical heat transfer model of actively cooled primary mirror of a solar telescope is proposed. The experimental validation has been carried out on the actively cooled honeycomb mirror with 600-mm diameter. When the temperature on the mirror surface fluctuates between 23.7 deg and 26 deg, the corresponding estimation error is not more than 0.4 deg. The experimental results validate the correctness and accuracy of the proposed method. [DOI: 10.1117/1.JATIS.3.4.046001]

Keywords: noncontact temperature estimation method; actively cooled primary mirror; large ground-based solar telescope.

Paper 17067 received Aug. 17, 2017; accepted for publication Oct. 13, 2017; published online Nov. 2, 2017.

1 Introduction

With the progress in solar physics, the higher temporal and spatial resolution for solar observation is required. Relative studies indicate that most scientific research focuses on a very small spatial scale of 50 to 100 km at the solar atmosphere, corresponding to an angle resolution of 0.1 arc sec.[1] Therefore, only a solar telescope with at least 1-m aperture can satisfy the latest solar physics research. For difficulties in sealing and stress birefringence of a large aperture window, open structure gradually replaces the traditional vacuum structure for telescopes with meter-sized aperture or above. However, for solar irradiance, the primary mirror is heated and its temperature difference with the ambient air will result in mirror seeing effect[2] and thermal deformation.[3]

To mitigate the mirror seeing effect and thermal deformation, the actively cooled primary mirror to control the mirror surface temperature is gradually being utilized in large ground-based solar telescopes. The actively cooled primary mirror has two types. One is the lightweight sandwich mirror,[4] the other is the active thin mirror.[5] The sketch of cooled system for two types of mirror is shown in Fig. 1. The absorbed heat transfer to the back surface of mirror and is cooled by the temperature-controlled air from the nozzle.

Currently, all the large ground-based solar telescopes in operation or under development, such as GREGOR (the German solar telescope with 1.5 m aperture),[4] Goode Solar Telescope (GST),[5] Daniel K. Inouye Solar Telescope (DKIST),[6] European Solar Telescope (EST),[7] National Large Solar Telescope (NLST),[8] and Chinese Large Solar Telescope (CLST),[9] are equipped with the actively cooled primary mirror. For a feedback control system, the surface temperature of primary mirror, which is the control objective, should be accurately detected.

Generally, there are two ways to detect the surface temperature of an object. One is the contact estimation method and the other is the noncontact estimation method based on infrared detection. However, due to the solar irradiance and fragility of the mirror surface coating, the contact temperature sensor cannot be adhered on the mirror surface directly. Also, the high reflectivity and the low infrared emissivity of the mirror surface coating make the infrared thermal imaging not available. As a compromise, the surface temperature of primary mirror is usually replaced by the temperature in the vicinity of the mirror surface, such as the back of the mirror face sheet or the shadows of the spiders on mirror surface,[10–12] where the traditional temperature estimation method is available. Therefore, how to accurately measure the temperature on the surface of an actively cooled primary mirror is still an unsolved problem.

In this paper, a surface temperature estimation method for actively cooled primary mirror surface is proposed. The proposed mirror surface temperature estimation method is based on the analytical heat transfer model of the actively cooled mirror. Furthermore, the experiment is carried out to validate the proposed temperature estimation method.

2 Analytical Heat Transfer Modeling of Actively Cooled Primary Mirror

2.1 *Heat Transfer Model of Primary Mirror*

For simplification, two types of actively cooled primary mirror can be simplified as the heat transfer model of plate with air jet impingement cooling (Fig. 2).[13,14]

The above simplified heat transfer model can be described by a one-dimensional (1-D) transient heat transfer model (Fig. 3).

The 1-D transient heat transfer partial differential equation is applied along the x-direction through the face sheet of primary mirror. For the front of the face sheet, there are convection with air, absorbed solar radiation, and thermal radiation with the environment. On the back of the face sheet, where the air jet impingement is formed, there is the forced convection between the air jet and the mirror and the thermal radiation with the

*Address all correspondence to: Changhui Rao, E-mail: Chrao@ioe.ac.cn

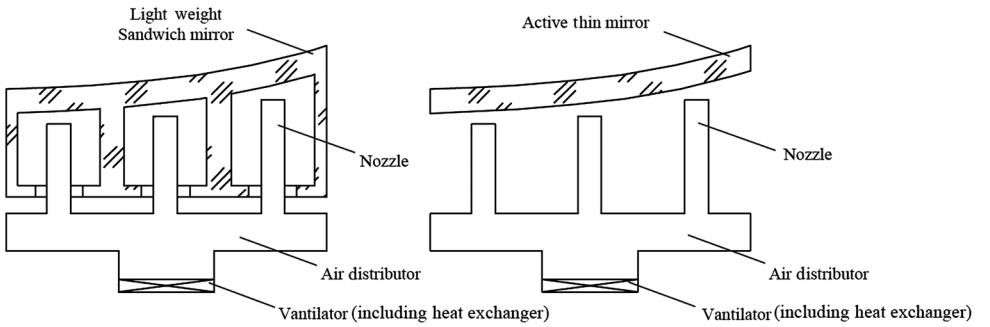

Fig. 1 Sketch of actively cooled primary mirror (a) lightweight sandwich mirror and (b) active thin mirror.

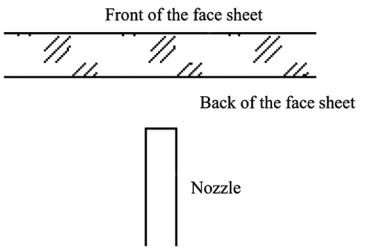

Fig. 2 Heat transfer model of plate with air jet impingement cooling.

environment. For lower temperatures and the emission rate of a coating with high reflectivity, the thermal radiation is neglected on both sides of face sheet. The heat transfer model of the face sheet of the actively cooled primary mirror is expressed as[15]

$$\begin{cases} k\frac{\partial^2 T(x,t)}{\partial x^2} = \rho C_p \times \frac{\partial T(x,t)}{\partial t}\,(t > 0, 0 \le x \le L) \\ -k \times \frac{\partial T(0,t)}{\partial x} = h_c \times [T(0,t) - T_c(t)] \\ -k \times \frac{\partial T(N,t)}{\partial x} = h_n \times [T(N,t) - T_{\text{amb}}(t)] + q(t) \end{cases}, \tag{1}$$

k, ρ, and C_p are the thermal conductivity, the density, and the specific heat of the mirror material, respectively. $T_c(t)$, $T_{\text{amb}}(t)$, and $q(t)$ are the outlet temperature of the air jet, the ambient temperature, and the absorbed solar radiation as functions of time, respectively. $T(x,t)$ is the temperature of x-position at time t. h_n and h_c are the heat transfer coefficients on the front and the back of the face sheet of primary mirror, respectively.

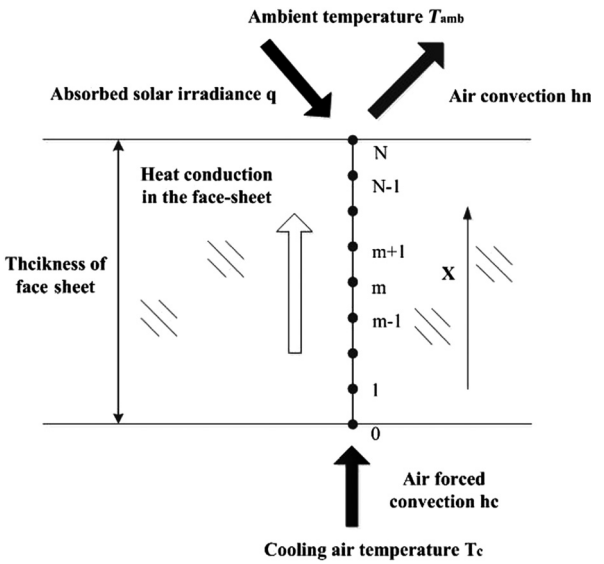

Fig. 3 1-D transient heat transfer model for the face sheet of the actively cooled primary mirror.

To solve Eq. (1), we discretize Eq. (1) in time and space domain. Central and forward differences are, respectively, applied for the second- and the first-order differential terms. For time stability of solution, the implicit scheme is used. The differential equations are given as

$$\begin{cases} k\left(\frac{T_{m-1}^{i+1} - 2T_m^{i+1} + T_{m+1}^{i+1}}{\Delta x^2}\right) = \rho C_p \frac{(T_m^{i+1} - T_m^i)}{\Delta t} \\ k\frac{(T_1^{i+1} - T_0^{i+1})}{\Delta x} + h_c(T_c^{i+1} - T_0^{i+1}) = \rho C_p \frac{\Delta x}{2}\frac{(T_0^{i+1} - T_0^i)}{\Delta t} \\ k\frac{(T_N^{i+1} - T_{N-1}^{i+1})}{\Delta x} + h_n(T_{\text{amb}}^{i+1} - T_N^{i+1}) + q = \rho C_p \frac{\Delta x}{2}\frac{(T_N^{i+1} - T_N^i)}{\Delta t} \end{cases}. \tag{2}$$

Equation (2) expressed in matrix forms is given as

$$AT = BC, \tag{3}$$

$$A = \begin{bmatrix} c & 2a & & & \cdots & & 0 \\ a & b & a & & & & 0 \\ 0 & a & b & a & & & \\ \vdots & & \ddots & \ddots & \ddots & & \vdots \\ & & & a & b & a & 0 \\ 0 & & & & a & b & a \\ 0 & & \cdots & & & 2a & e \end{bmatrix}_{(N+1)\times(N+1)},$$

$$T = \begin{bmatrix} T_0^{i+1} \\ T_1^{i+1} \\ \vdots \\ T_{m-1}^{i+1} \\ T_m^{i+1} \\ T_{m+1}^{i+1} \\ \vdots \\ T_{N-1}^{i+1} \\ T_N^{i+1} \end{bmatrix}_{(N+1)\times 1}, \tag{4}$$

$$B=\begin{bmatrix} -1 & 0 & & & & 0 & 0 & -d \\ 0 & -1 & & & & 0 & 0 & 0 \\ & & \ddots & & & \vdots & \vdots & \vdots \\ & & & -1 & 0 & 0 & 0 & 0 \\ & & & 0 & -1 & -f & -g & 0 \end{bmatrix}_{(N+1)\times(N+4)},$$

$$C=\begin{bmatrix} T_0^i \\ T_1^i \\ \vdots \\ T_{m-1}^i \\ T_m^i \\ T_{m+1}^i \\ \vdots \\ T_N^i \\ T_{amb}^i \\ q^i \\ T_c^i \end{bmatrix}_{(N+4)\times 1}, \tag{5}$$

$$a=\tau=\frac{k\Delta t}{\rho C_p \Delta x^2}, b=-(1+2\tau),$$
$$c=-\left(1+2\tau+2\tau\frac{\Delta x\cdot h_C}{k}\right) d=2\tau\frac{\Delta x\cdot h_C}{k},$$
$$e=-\left(1+2\tau+2\tau\frac{\Delta x\cdot h_n}{k}\right), f=2\tau\frac{\Delta x\cdot h_n}{k}, g=2\tau\frac{\Delta x}{k},$$
$$\tau=\frac{k}{\rho C_p}\times\Delta t/\Delta x^2, \Delta x=\frac{L_{\text{thickness}}}{N}, \tag{6}$$

where $L_{\text{thickness}}$ is the thickness of the face sheet and N is the number of nodes along the x-direction. Using the inverse of matrix A, Eq. (7) is obtained

$$\mathrm{T}=A^{-1}BC. \tag{7}$$

Matrix T represents the temperature distribution along the x-direction at the next moment. Using Eq. (7), the temperature distribution at any time can be obtained.

2.2 *Heat Transfer Coefficient on the Front of the Face Sheet*

The convection on the front of the face sheet is equivalent to the forced cooled model of a flat plate. In the model, the diameter of a round plate is the characteristic length.

According to the experiments,[15] Eqs. (8)–(10) are obtained

$$Nu_L=\frac{h_n L}{\lambda}=0.664Re_L^{1/2}Pr^{1/3}, \quad (Re_L\le 5\times 10^5), \tag{8}$$

$$Nu_L=\frac{h_n L}{\lambda}=0.037(Re_L^{4/5}-871)Pr^{1/3}, \quad (Re_L>5\times 10^5), \tag{9}$$

$$Re_L=\frac{u_L L}{\nu}. \tag{10}$$

The heat transfer coefficient h_n on the front of the face sheet can be calculated. Re_L is the Reynolds number, which is decided by the flow velocity u_L (unit: m/s), the diameter of plate L (unit: m), and the dynamic viscosity ν (unit: m^2/s). Nondimensional parameters Pr and Nu_L are the Nusselt number and the Prandtl number, respectively. λ [unit: $W/(m\cdot K)$] is the thermal conductivity of the air flow.

2.3 *Heat Transfer Coefficient on the Back of the Face Sheet*

The air jet-cooled system on the back of the face sheet is equivalent to the single round air jet-cooled model (Fig. 4).

The h_c is the heat transfer coefficient on the back of the face sheet. The mean heat-transfer coefficient h_c in the jet zone of radius r is expressed as[15]

$$\frac{h_c D}{\lambda}=(Nu_D)_M$$
$$=2Re_D^{0.5}Pr^{0.42}(1+0.005Re_D^{0.5})^{0.5}\times\frac{1-1.1D/r}{1+0.1(H/D-6)D/r}\frac{D}{r}, \tag{11}$$

$$Re_D=\frac{u_D D}{\nu}, \tag{12}$$

where D, H, and r (unit: m) are the dimensions as shown in Fig. 4. Nondimensional parameters $(Nu_D)_M$, Re_D, and Pr are the mean Nusselt number, the Reynolds number with characteristic length D, and the Prandtl number of air. h_c and λ are the mean heat transfer coefficients on the plate and the thermal conductivity of the air jet.

Equation (11) is validated by the experiments when it satisfied the conditions as

$$2\times 10^3\le Re_D\le 4\times 10^5, 1\le\frac{H}{D}\le 12, 2.5\le\frac{r}{D}\le 7.5. \tag{13}$$

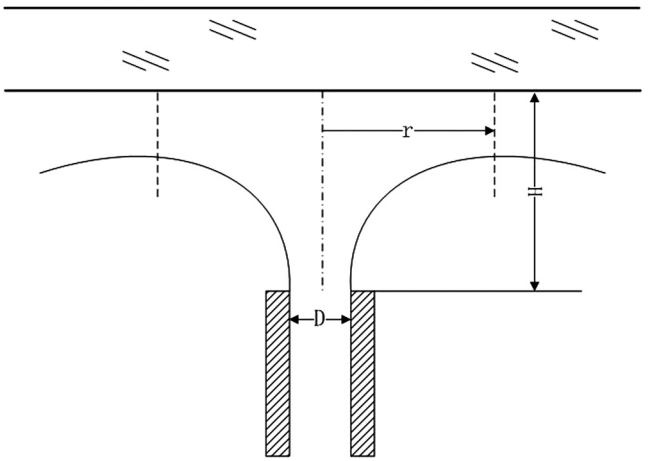

Fig. 4 A single round jet-cooled model.

3 Noncontact Surface Temperature Estimation Method on Actively Cooled Primary Mirror Based on the Heat Transfer Model of the Mirror Face Sheet

The noncontact surface temperature estimation method is based on the heat transfer model of actively cooled primary mirror face sheet. The proposed estimation method includes the following steps:

a. Ambient parameters definition: Sensors are used to measure the ambient air temperature (denoted as T^i_{amb}, unit: K), the outlet air jet temperature of nozzle (denoted as T^i_c, unit: K), the solar irradiance (denoted as q^i, unit: W/m^2), and the ambient air velocity (denoted as u^i_L, unit: m/s). The sampling period of these sensors is denoted as Δt.

b. Mirror parameter definitions: The heat conductance, the specific heat, and the density of mirror material are, respectively, denoted as k (unit: W/mK), C_p (unit: J/kg K), and ρ (unit: kg/m^3). The thickness of the mirror face sheet is $L_{\text{thickness}}$ (unit: m).

c. The heat transfer coefficient on the front face sheet is obtained from a look-up table: based on the measured ambient temperature T^i_{amb}, the dynamic viscosity, and the thermal conductance and the Prandtl number of the ambient air is obtained by looking-up table. Substituting these parameters into Eqs. (8)–(10) produce the heat transfer coefficient on the front of the face sheet, which is denoted as h_n (unit: W/m^2 K).

d. The heat transfer coefficient on the back of the face sheet is obtained from a look-up table: Based on the measured outlet air jet temperature of nozzle T^i_c, the dynamic viscosity, and the thermal conductance and the Prandtl number of the ambient air is obtained by looking-up table. Additionally, the inner diameter, the gap between the outlet of the nozzle and the back of mirror face sheet, and the radius of the jet zone (mirror cell) are, respectively, denoted as D (unit: m), H (unit: m), and r (unit: m). Substituting these parameters into Eqs. (11)–(13) produce the heat transfer coefficient on the back of the face sheet, which is denoted as h_c (unit: W/m^2 K).

e. Mirror surface temperature calculation: Substituting the above parameters into Eq. (7) produce the estimated surface temperature T^{i+1}_N of actively cooled primary mirror.

In the next section, the proposed temperature estimation method is experimentally validated in a specific actively cooled primary mirror.

4 Experimental Validation

4.1 *Prototype of Chinese Large Solar Telescope and Its Actively Cooled Primary Mirror*

To fill the gap of high-resolution solar observation in east Asia, China is planning to build a CLST with 1.8-m aperture.[16–18] To validate a series of key technologies including the actively cooled primary mirror, the Prototype of Solar Telescope (POST) has been built[19] (Fig. 5).

The primary mirror of the POST is an actively cooled honeycomb mirror made of ultralow expansion glass (ULE, Table 1). The diameter L and the thickness $L_{\text{thickness}}$ of the primary mirror are 600 and 20 mm, respectively. The inner diameter D of nozzle and the gap H between nozzle and plate are 15 and 20 mm (Fig. 4), respectively. The radius r of inscribed circle of hexagon cell is 45 mm.

The thermal control system for honeycomb primary mirror of the POST is shown in Fig. 6.

Air jet impingement cools the back of the face sheet of primary mirror directly. Refrigerator and electrical heater collaboratively work to regulate the cooling air temperature to realize the active thermal control of the primary mirror surface. The ventilator works at a fixed frequency, and the mean outlet velocity of nozzles u_D is 3.16 m/s. Experimental measurements of the air jet flow rate differences for the nozzles are <5%. For mirror temperature measurement, two temperature sensors are installed at the outlet of nozzle (S1) and the front of the face sheet corresponding to the same cell [S2, Fig 7(a)]. Temperature sensor S3 is used to measure the ambient temperature. After the calibration and modification, the maximum measurement error of each temperature sensor is <0.05 deg.

4.2 *Experimental Results*

To validate the proposed temperature estimation method, a laboratory experiment has been carried out. Since there is no solar

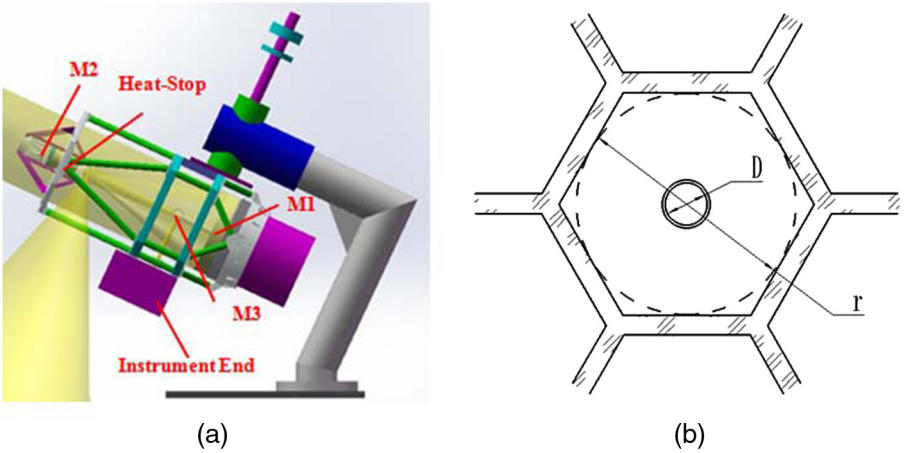

Fig. 5 (a) Three-dimensional sketch of POST and (b) cross section of POST primary mirror cell.

Table 1 Properties of the ULE.

Property	Value
Density (kg/m^3)	2210
Thermal conductivity (W/m K)	1.31
Specific heat (J/kg K)	766

irradiance in the room, the absorbed solar irradiance q^i equals zero. To test the thermal response of the primary mirror in the room, the refrigerator and electrical heater work alternately to produce the temperature fluctuation. The ambient temperature of the laboratory is not controlled. The following temperatures are measured: the variation in the temperature of the environment (temperature sensor S3), the front-sheet (temperature sensor S2), and the air jet in the cell (temperature sensor S1). These are identified in Fig. 6 and their variations versus time are shown in Fig. 8.

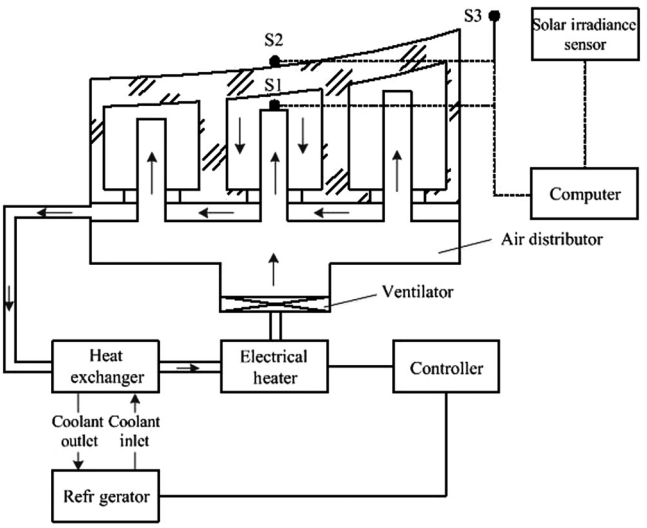

Fig. 6 Thermal control system for primary mirror of the POST.

For the small temperature range (<5 deg) and the low humidity of the air in the room (the dehumidification is on), the properties of dry air are assumed as constant quantities. Refer to the dry air at 25 deg,[15] the properties are shown in Table 2. The velocity of ambient air flow u_L in the room is about 0.1 m/s (tested by the hot-wire anemometer of TESTO 425).

Substituting the parameters into Eqs. (8)–(11), the heat transfer coefficients on the front of the face sheet and the back of the face sheet are 1.6 and 47 W/m^2 K, respectively.

The number of nodes N is set as 20. For the sampling, frequency of temperature sensor is 0.2 Hz, the corresponding time step Δt equals 5 s. Substituting the measured temperature into series of the environment (measured by temperature sensor S3) and the air jet in the cell (measured by temperature sensor S1) into Eq. (7), the measured temperature on the front of the face sheet is obtained (Fig. 9). Here, the calculated temperature series is the result of the proposed noncontact temperature estimation method.

To validate the proposed estimation method, the calculated result is compared with the real temperature on the mirror (measured by temperature sensor S2). The estimation error is defined as

$$\text{error}_{\text{absolute}}(N) = T_{\text{experimental}}(N) - T_{\text{theory}}(N). \tag{14}$$

The estimation error with time variations is shown in Fig. 10.

Figure 10 shows that the error is no >0.4 deg. In the meanwhile, the mean value of the error is 0.14 deg. Based on the analysis, the acceptable temperature rise on mirror surface should be within 2 deg.[20] Therefore, the error of the proposed noncontact temperature estimation method is acceptable.

(a) (b)

Fig. 7 (a) The temperature sensor S2 for experimental validation on the mirror surface (the probe is in the circle) and (b) the photo of the POST after assembly.

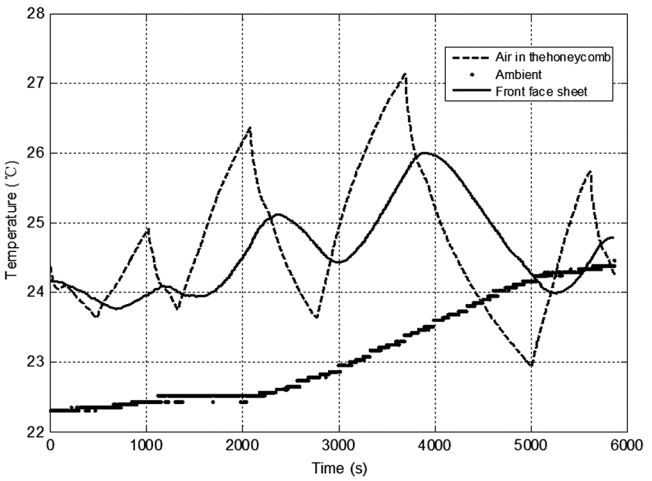

Fig. 8 Temperature with time variation of in-room experiment.

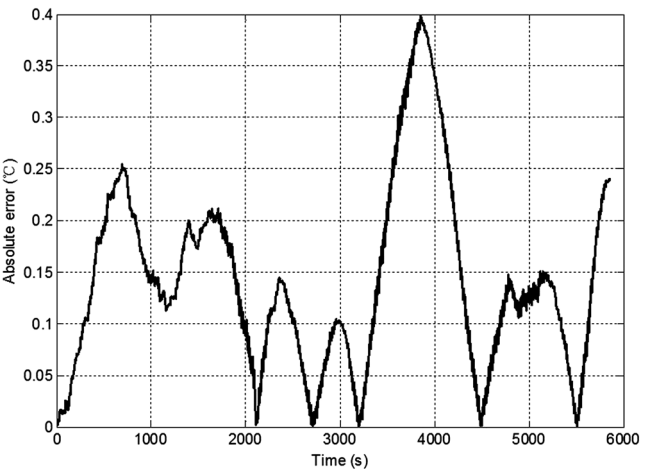

Fig. 10 Error of theoretical temperature curve.

Table 2 Properties of the dry air at 25 deg.

Property	Value
Dynamic viscosity (unit: m^2s)	15.71×10^{-6}
Thermal conductivity [unit: (W/m K)]	26.14×10^{-3}
Prandtl number	0.707

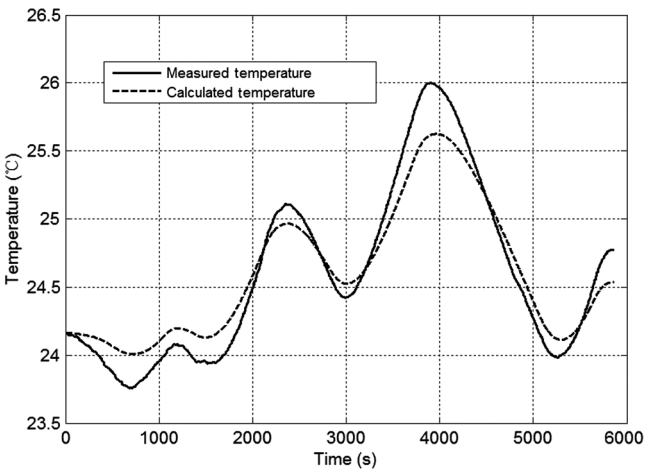

Fig. 9 Temperature curve of theoretic and experimental results.

5 Summary and Conclusions

In this paper, a noncontact temperature estimation method based on the analytical heat transfer model for actively cooled primary mirror is proposed. To validate the method, the experiment based on the prototype POST has been carried out. Using this method, the surface temperature on the actively cooled primary mirror surface can be obtained without traditional temperature measurement methods.

Acknowledgments

We would like to express our gratitude to Mrs. Cheng Li, Dr. Lei Zhu, Dr. Lanqiang Zhang, Mr. Jinlong Huang, Mr. Yuntao Chen, Mr. Benxi Yao, and Mr. Zhiyong Wang from Institute of Optics and Electronics, Chinese Academy of Sciences, for their help. A special acknowledgement should be shown to Professor Wenhan Jiang from the Institute of Optics and Electronics, Chinese Academy of Sciences, for his revision we benefited greatly. This work was funded by the National Natural Science Foundation of China (Nos. 11727805 and 11733005).

References

1. R. Volkmer et al., "Progress report of the 1.5 m solar telescope GREGOR," *Proc. SPIE* **5489**, 693 (2004).
2. M. K. Cho, J. DeVries, and E. Hansen, "Thermal performance of the ATST secondary mirror," *Proc. SPIE* **6721** 672102 (2007).
3. R. K. Banyal, B. Ravindra, and S. Chatterjee, "Opto-thermal analysis of a lightweighted mirror for solar telescope," *Opt. Express* **21**(6), 7065–7081 (2013).
4. O. Von Der Lühe et al., "GREGOR: a 1.5 m telescope for solar research." *Astron. Nachr.* **322**, 353–360 (2001).
5. L. V. Didkovsky, J. R. Kuh, and P. R. Goode, "Optical design for a new off-axis 1.7 m solar telescope (NST) at big bear," *Proc. SPIE* **5171**, 333 (2004).
6. J. Wagner et al., "Advanced technology solar telescope: a progress report," *Proc. SPIE* **7012**, 70120I (2008).
7. R. Volkmer et al., "EST telescope primary mirror, support and cooled system," *Proc. SPIE* **7739**, 77391O (2010).
8. S. S. Hasana et al., "NLST—the Indian national large solar telescope," *Proc. SPIE* **7733**, 77330I (2010).
9. C. Rao et al., "1.8-m solar telescope in China: Chinese large solar telescope," *J. Theor. Appl. Inf. Technol.* **1**(2), 024001 (2015).
10. P. Emde et al., "Thermal design features of the solar telescope GREGOR," *Proc. SPIE* **5495**, 238 (2005).
11. R. Volkmer, "Thermal characteristics of the solar telescope GREGOR," *Proc. SPIE* **7012**, 70120K (2008).
12. R. Volkmer et al., "GREGOR telescope—start of commissioning," *Proc. SPIE* **7733**, 77330K (2010).
13. R. Volkmer et al., "Optical and thermal design of the main optic of the solar telescope GREGOR," *Proc. SPIE* **5179**, 270 (2010).
14. E. Hansen, R. Price, and R. Hubbard, "Advanced technology solar telescope optical design," *Proc. SPIE* **6267**, 62673Z (2006).
15. S. Yang and W. Tao, *Heat Transfer*, Vol. **2**, pp. 311–315, Higher Education Press, Beijing (2006).
16. C. Rao et al., "1.8-M solar telescope in China: the CLST," *Proc. SPIE* **9145** 914529 (2014).

17. Y. Liu, N. Gu, and C. Rao, "Quantitative evaluation on internal seeing induced by heat-stop of solar telescope," *Opt. Express* **23**(15), 19980–19995 (2015).
18. Y. Liu et al., "A heat-stop structure design with high cooled efficiency for large aperture size ground based solar telescope," *Appl. Opt.* **54**(21), 6441–6447 (2015).
19. Y. Liu et al., "Active thermal control for the 1.8-m primary mirror of the solar telescope CLST," *Proc. SPIE* **9906**, 99061C (2016).
20. P. Emde et al., "Thermal design features of the solar telescope GREGOR," *Proc. SPIE* **5495**, 238 (2004).

Yangyi Liu received his PhD in optical engineering from the Institute of Optics and Electronics, Chinese Academy of Sciences, in 2016. His interests are mainly in thermal control technology of solar telescope and postfocus instruments currently. He is also the main member of Chinese Large Solar Telescope group on its thermal control system.

Naiting Gu received his MS and PhD degrees in optical engineering from the Institute of Optics and Electronics, Chinese Academy of Sciences, in 2009 and 2012, respectively. He has researched on wavefront measurement technology and interferometry imaging technology for several years. Currently, he devotes himself to observe the solar activity, including solar observation facility, solar adaptive optics, and postfocus instruments.

Changhui Rao is the member of SPIE and OSA. He has been engaged in the research on adaptive optics and optical propagation through atmosphere for more than 20 years. More than 200 papers have been published. He is also the vice director of the Institute of Optics and Electronics and the vice director of the Key Laboratory on Adaptive Optics.